Sparse array techniques for 2D array ultrasound imaging

Bakary Diarra, Hervé Liebgott, Piero Tortoli, Christian Cachard

ACOUSTICS 2012

Sparse array techniques for 2D array ultrasound imaging

B. Diarra[a,b], H. Liebgott[a], P. Tortoli[c] and C. Cachard[a]

[a]Centre de recherche en applications et traitement de l'image pour la santé, 7 avenue Jean Capelle, Bat Blaise Pascal, 69621 Villeurbanne Cedex
[b]Department of Electronics and Telecommunications [Florence], Via S. Marta, 3 50139 Firenze
[c]Università degli studi di Firenze, Via S. Marta, 3, 50139 Firenze, Italy
bakary.diarra@creatis.univ-lyon1.fr

Ultrasound imaging is the cheapest and the most secure imaging modality used in every day diagnosis. One of the most attractive ultrasound fields in recent years is three dimensional imaging with 2D matrix probe. The difficulty to realize these probes comes from the huge number of elements necessary to its composition. In our application, the probe is composed of 1024 elements (64x16) which are too many for most of the current beamformers that have usually 64 to 256 channels. Many techniques are proposed in literature to reduce the necessary active elements to be connected in the 2D array to preserve its beam characteristics. The paper presents one of these techniques known as the sparse array. Both the regular and the random configurations of this method are tackled. The simulated annealing algorithm is combined to the random sparse array to efficiently reduce the initial 1024 elements by minimizing the effect of side lobes on the resulting beam pattern. The probe is intended to be suitable for needle tracking during hepatic biopsy and therapy applications. It can also be used in other micro-tools or internal organs operations.

1 Introduction

In 3D ultrasound imaging, the experiments are mostly conducted with 3D mechanical probes. It would be extremely interesting to work with 2D matrix arrays electronically controlled. However the control of such arrays is a technical challenge because of their huge number of elements that makes difficult their connections. These arrays are under study since many years but till now there are still not used in clinical routine. Many methods have been studied to reduce the number of elements and the most efficient one is the sparse array technique [1]. This later does not present only advantages; it deteriorates the beam pattern compared to the dense array. After the element number reduction, a beam pattern optimization is necessary to correct some of the drawbacks, mainly the side lobes apparition.

In a recent publication [2] our team has presented the results of an algorithm for needle detection in 3D mechanical ultrasound data. The detection algorithm based on a RANSAC procedure is fast and accurate but the volume acquisition time is a limitation for this application. The 2D array imaging is a solution to this limitation and that is why we propose a method to design a 2D sparse matrix array for hepatic biopsy. The dimensions of the probe are chosen in accordance to inter-costal distance.

The simulation results presented in this work proves the feasibility of this probe for liver imaging.

The paper is organized as follows: in section 2 the state of art in the 2D array domain is described, the explanation of the new method and the section III the characteristics of the biopsy probe considered. The sections IV and V are respectively sparse techniques the discussion and the conclusion.

2 State of art

B mode imaging with 1D array probes presents many limitations in human tissue representation. The real structures are three dimensional geometries and 1D probes just produce thin sliced planes at a given angle and it is difficult to localize and reproduce the same plane at a later time for follows-up studies [3]. This makes compulsory to the physician to memorize several 2D planes to reconstruct the entire observed structure. To overcome these limitations, 3D imaging using 1D arrays controlled mechanically to sweep the third spatial dimension has been developed. This imaging modality is based on linear or rotational displacement of a 1D probe to collect several 2D imaging planes for an image volume reconstruction. These volumes represent more correctly the human anatomy than individual 2D images which compose them. 3D mechanical imaging has been used in obstetrics for fetus evolution status viewing, in cardiology, in abdominal imaging [3], in surgical tools tracking [2]. Although 3D mechanical imaging overcomes some limitations of the classical 2D imaging, it presents its own limitations. It has a poor resolution in elevation direction and the volume reconstruction operation is very time consuming, this impedes this 3D imaging to be used in real time needed surgical operations imaging. So that, for needle detection (biopsy) or any surgical tool tracking 3D mechanical imaging will not be the best solution.

All these quoted limitations lead researchers to investigate a new kind of imaging probes: 2D arrays which are matrices of elements. Such kind of probes provides a solution to the elevation resolution problem because of their capability to focus ultrasonic beams in the two directions (elevation and lateral). Moreover they can produce real time volumetric images under some conditions. The 2D arrays do not present only advantages. The main difficulty is the technological aspect; a mean 2D array contains hundreds or even thousands of elements to be connected. This important element number poses a serious problem to the realization and so the everyday use of these probes. Many solutions were considered by the researchers to overcome this obstacle. The multiplexing can be used to connect by turns all the elements if the real time nature is not essential for the targeted application. This is the case in the 2D array synthetic aperture imaging as described in some studies presented in [4][5]. For the real time feasibility all the probe elements must be connected simultaneously to scan the entire volume in the same beamforming operation. To satisfy these conditions several methods such as sparse array [1][6], spiral array [7], row-column addressing [8] were investigated. Many studies about the sparse array were realized with roughly the same conclusion, that is the side lobes apparition, main lobe widening, and resolution loss [1][6].

3 Probe design and parameters

The main parameters of the probe are chosen based on the characteristics of the environment of the organ to be explored, which is the liver in this application. The frequency commonly used in liver imaging is 3.5 MHz [9] and this corresponds to a wavelength (λ) of 0.44 mm. To avoid grating lobes apparition the pitch value should not exceed a mid-wavelength but this condition also increases the main lobe width. A value slightly above the mid-wavelength is a good tradeoff and the pitch is chosen to be $d = 0.6\lambda$. The elements are squared and their size is $w_d = 0.5\lambda$ and the kerf $= 0.1\lambda$. The probe elevation dimension must be smaller than the inter-costal distance, which is about 5 mm, to avoid the reflection on ribs and the formation of image artifacts. With such a pitch the number of elements rows in the elevation direction is 22. For electronic adaptability this number is chosen to be 16. The number of elements in lateral direction is 64, currently used as selected elements number of a linear phased array, so the resulting probe contains N=64x16=1024 elements. These are too many elements to connect because the typical channel number of beamformers doesn't exceed 128; consequently N has to be decreased without too much deterioration on the imaging features. The beam profiles of the 2D array are obtained by simulation with Field II [10][11]. All the beam profiles presented in this paper are obtained by plotting the maximum pressure of each A-line of the volume scanned in both lateral and elevation direction. As the probe is not square, the beam is not the same in the two directions.

Figure 1:64x16 2D array probe parameters

4 Sparse array techniques

To resolve the difficulty linked to the huge number of elements in the 2D array and make easy their use with the recent beamformers, the sparse array is the most promising solution among a mountain of approaches proposed in the literature [1][6].

Before using the sparse array, we can opt for the reduced dense array as proposed by Turnbull *et al* [1]. This technique consists in deactivating the edge elements and activating only the circular (or elliptic for non-squared array) part of elements matrix. Moving from a square (or rectangular) aperture to a circular one reduces elements number of about 20% of the initial element [12] to 30% [13].

The initial array containing 1024 elements was reduced to 728 elements (29% lower). This reduction doesn't affect because of the weak contribution of these edge elements in the resulted beam pattern (Figure 2). This reduced form will be used in the sparse array techniques presented in this paper.

The beam profiles presented in Figure 2(as all the other beam profiles) in this paper are obtained by plotting the maximum pressure of each A-line in lateral and elevation direction. Because of the symmetry of the beam profile, only its right part is plotted.

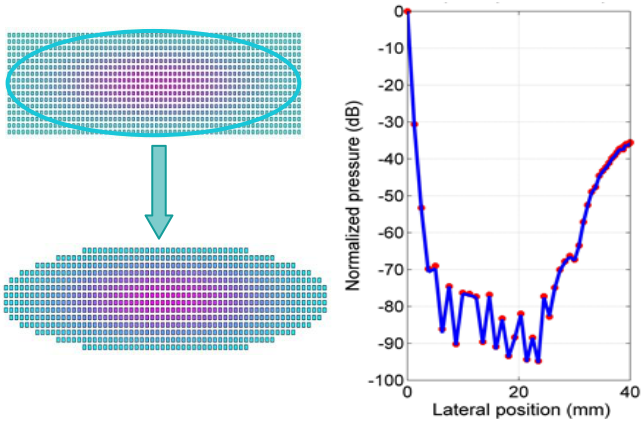

Figure 2: simulation at 40 mm depth: 2D array beam conservation before (continuous line) and after (dotted line) the corner elements deactivation

4.1 Regular sparse array

The regular (or periodical) version is obtained by periodically activation of a precise number of elements. This method presents a good beam pattern in terms of main lobe width and pressure intensity and its permits a good reduction in the element number. Its main drawback is the grating lobes apparition due to the array periodicity (Figure 3 d, e, and f). The grating lobes come from the spatial sampling of the element in the probe when the elements size is larger than the mid-wavelength (as Shannon condition in signal processing). The Figure 3 represents three different configurations of the regular sparse array presented by Austeng et al [12]. The first configuration Figure 3a) is obtained by activating one element out of two, the second Figure 3b) by activating two elements out of three and the last one Figure 3c) by activating one element out of three. This gives 2D arrays which pitches are larger than the initial probe pitch shown in Figure 1). This increase of the pitch leads to high grating lobes which are too close to the main lobe. To minimize the effect the grating lobes, the concept of effective aperture is sometimes used.

The effective aperture is a concept applied to the sparse periodic arrays. This concept consists in emitting with a configuration and receiving with another in the manner that the side lobes in emission correspond to the zeros of the pressure profile of the reception [12][14]. In most of time no element must be common to both transmission and reception aperture but some exceptions exist [14]. The same concept with some light modifications is called coarray in [15]. The results when using this concept in the grating lobes reduction purpose are shown by Figure 4. The emission uses the 2D array of Figure 3a) and the reception uses respectively the same 2D array, the one of Figure 3b) and Figure 3c). As the grating lobes positions of Figure 3a) are different of that of

Figure 3b and c), the resulting beam profile has much low grating lobes (Figure 4 full dotted line and dashed dotted line). The difficulty of the regular sparse array use in the practical case comes from the constraint to have two different 2D arrays in emission and in reception to perform a good beam pattern.

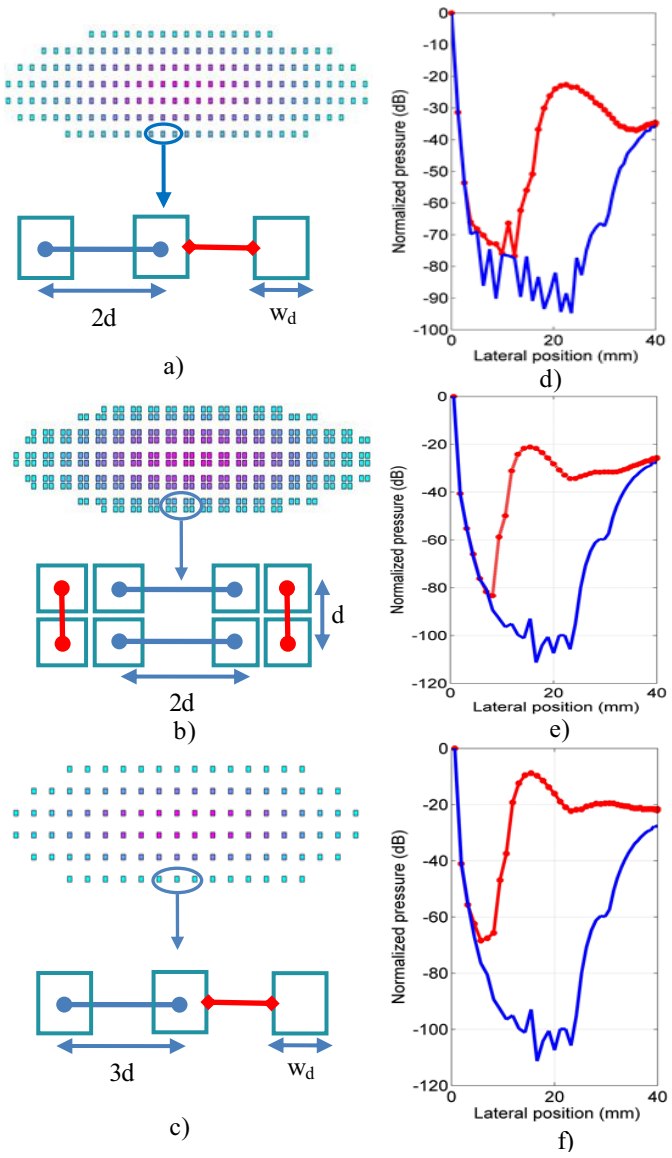

Figure 3: regular sparse array configurations a) with ½ active elements (256) , b) 2/3 active elements (334), c) 1/3 active elements (132) and respectively d) , e) and f) their beam profiles (dotted line) compared to the dense array's one (continuous line)

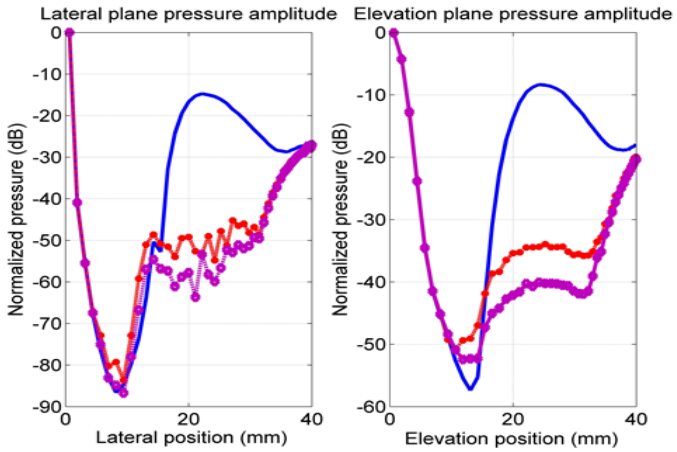

Figure 4: emission with ½ active elements probe and reception with the same array (continuous line), with a 1/3 active elements probe (continuous dotted line) and with a 2/3 active elements array (dashed dotted line)

4.2 Random sparse array

The random version is the most promising reduction technique among all other studied because of its presents the good tradeoff between the grating lobes and the active elements number comparing to the regular one. In this later the grating lobes have the same level as in the dense array but its drawback is due to another unwanted phenomenon which is the side lobes (local maxima in undesired direction). In the example of Figure 5a), the 2D array is filled with 256 active elements randomly placed within the array. The Figure 5b) illustrates the apparition of the side lobes when the active element decreases in the random sparse technique. As the activation of the element is random, it is possible to use an optimization algorithm to minimize both the element number and the side lobes level. In this purpose some studies used the simulated annealing algorithm[16] and the genetic algorithm [17]. In this paper the simulated technique is used to minimize the side lobes level and to avoid the main lobe widening as presented in [16][13].

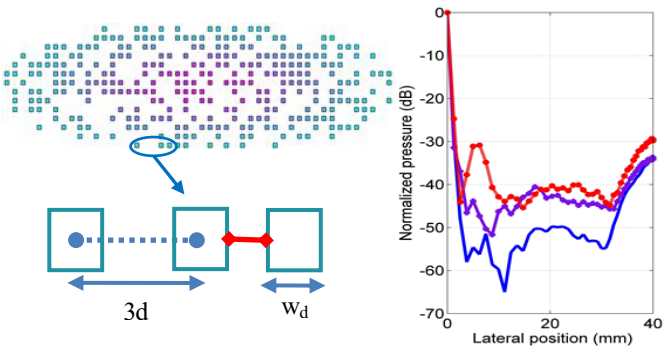

Figure 5: random sparse array beam profiles with 256 (continuous line), 180 (continuous dotted line) and 110 elements (dashed dotted line)

4.3 Optimized sparse array

The simulated annealing algorithm derived from the Metropolis algorithm [18] which was used in substances crystallization process to superimpose a cooling profile to the material. Kirkpatrick adapted the method to informatics problem optimization like the sparse array [19]. It is an iterative algorithm which perturbs the considered parameter's value at each iteration. The algorithm begins with the initial values of the temperature (term used in reference to [18]) and the parameters of the cost function. The simulated annealing proceeds by jumping from the last value of the parameter to its neighbor (value disturbance). The temperature is high at the beginning, so any new value of the parameter can be easily accepted because the probability of acceptance of a new state is close to 1. The generation of the new value x' of x was described in [19] by (2).

$$p_r(x = x') = \begin{cases} e^{(E'-E)/kT} & \text{if } E' > E \\ 1 \end{cases} \quad (1)$$

E' is the energy of the new state x' and E is the energy of the current state x, k is the Boltzmann constant and T is the temperature of the current iteration given by (2)

$$T_i = 0.9^i T_0 \quad (2)$$

In 2D sparse array, as there are many possible positions for a randomly selected element, it will be interesting to find the most suitable one to minimize the inter-element distance effect on the beam. The performance criteria of the algorithm are based on the - 6 dB bandwidth, the side lobes level (- 40 dB in this case) and the main beam width. Any overlapping between elements is not accepted [6][20].

The optimization procedure with the simulated annealing is made by a cost function (4) which contains all the parameters to be optimized. The element number and the side lobes level are the main variables to be optimized. A general notation of this function was used in [21] [16]. This function uses the pressure formulation established for the far field beam pattern by Nielsen et *al* [22]

$$p(u,v) = \left| \sum_{i=1}^{M} \sum_{j=1}^{N} w_{i,j} \cdot e^{-j\frac{2\pi}{\lambda}(x_i \cdot u + y_j \cdot v)} \right| \quad (3)$$

$w_{i,j}$ coefficient of the element at position (i, j)
x_i, y_j coordinates of the element at position (i, j)
u, v beam direction vectors

This beam function is used to fix the side lobes level in the desired area. The global final function was expressed by Trucco *et al* [16] and by Chen *et al* [21]

$$f(M) = k_1 \left[\sum_{(u,v) \in S} \left(\frac{p(u,v)}{A} - p_d(u,v) \right) \right]^2 + k_2 M^2 \quad (4)$$

A maximum of pressure
p_d desired side lobes level to be obtained
S area excluding the main lobe
M active elements' number
k_1, k_2 coefficients showing the terms importance in f

The area S reserved to the main lobe depends on the application and the author's choice. A completed study of the simulated annealing was detailed in [23][24].

4.4 Result of the array optimization

The beam profile of the dense array, used as the gold standard, is compared to that of 2D array optimized by simulated annealing (Figure 6). The 1024-element initial 2D array was reduced to 235 elements (77%) with good imaging features. The initial temperature value is T_0=1000 and the coefficients $k_1 = 5000$ and $k_2 = 0.2$. The main lobe widening in sparse array is overcome through the optimization, its value remains 0.2 mm at -6 dB (Figure 6c). The side lobes are lower than -40 dB too. The profile presented is obtained at a 40 mm depth.

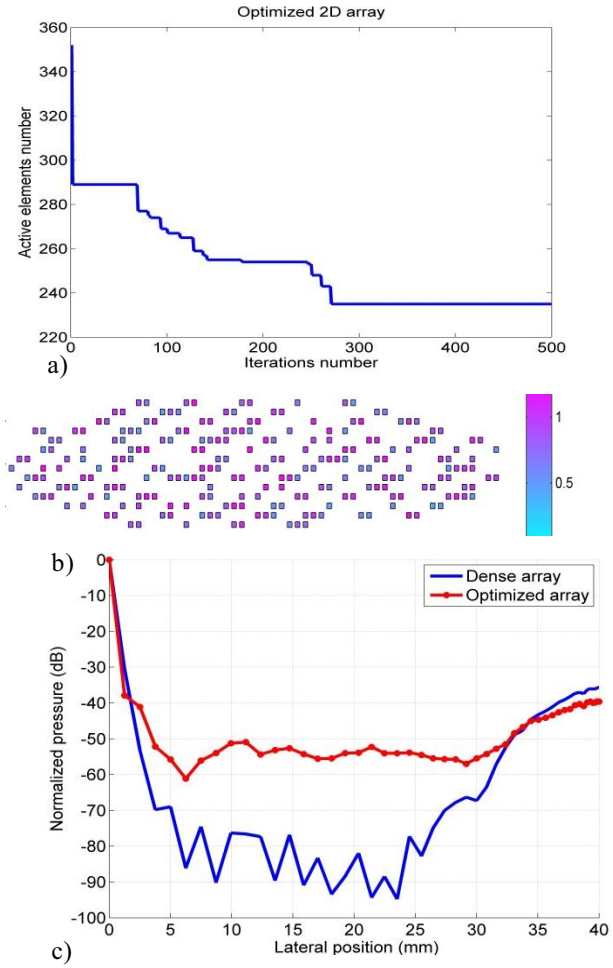

Figure 6: a) active element number as a function of the iterations b) optimized array c) beam profiles of the dense array (continuous line) and the optimized array (dotted line)

The beam profile of the optimized 2D array in Figure 6c) follows as well the one of the dense array till the -40 dB level with even a thinner main lobe between 0 and -40 dB.

5 Discussion and conclusion

The probe study in this paper fits to the targeted application. The sparse array beam profile presents a beam width larger than the one of the dense array because an important part of the energy is spread out the entire volume. The inter-elements distance plays a significant effect on the beam profile. The simulated annealing permits to have a good tradeoff between the number of element and the beam profile by an optimization process. We focus on the elements number minimization and the side lobes level reduction. The main lobes width at – 6 dB are 0.2 mm, as the needle medium radius is about 0.3 mm these results are acceptable for biopsy operations.

The beam profile of the optimized probe confirms that its fits well to biopsy applications. We will work to more reduce the elements number in the next step of our study by adopting a new strategy of elements placement into the probe and by modifying the cost function used to have a most efficient optimized probe.

Acknowledgments

Special thanks are extended to Labex CeLya for financial support. The main author is financially supported by the Franco-Italian University with a VINCI and a Galilee grant and by the Rhone-Alpes region with an Explora'Doc grant.

References

[1] D. H. Turnbull et F. S. Foster, « Beam steering with pulsed two-dimensional transducer arrays », *Ultrasonics, Ferroelectrics and Frequency Control, IEEE Transactions on*, vol. 38, n°. 4, p. 320–333, 1991.

[2] M. Uherčík, J. Kybic, H. Liebgott, et C. Cachard, « Model Fitting Using RANSAC for Surgical Tool Localization in 3-D Ultrasound Images », *Biomedical Engineering, IEEE Transactions on*, vol. 57, n°. 8, p. 1907–1916, 2010.

[3] A. Fenster, D. B. Downey, et H. N. Cardinal, « Three-dimensional ultrasound imaging », *Physics in Medicine and Biology*, vol. 46, n°. 5, p. R67, 2001.

[4] N. M. Daher et J. T. Yen, « 2-D array for 3-D Ultrasound Imaging Using Synthetic Aperture Techniques », *IEEE Trans Ultrason Ferroelectr Freq Control*, vol. 53, n°. 5, p. 912–924, mai 2006.

[5] A. . Fernandez, K. . Gammelmark, J. . Dahl, C. . Keen, R. . Gauss, et G. . Trahey, « Synthetic elevation beamforming and image acquisition capabilities using an 8 × 128 1.75D array », *Ultrasonics, Ferroelectrics and Frequency Control, IEEE Transactions on*, vol. 50, n°. 1, p. 40 – 57, janv. 2003.

[6] P. K. Weber, R. M. Schmitt, B. D. Tylkowski, et J. Steck, « Optimization of random sparse 2-D transducer arrays for 3-D electronic beam steering and focusing », in *Proceedings of IEEE Ultrasonics Symposium*, Cannes, France, 1994, vol. 3, p. 1503–1506.

[7] T. S. Sumanaweera, J. Schwartz, et D. Napolitano, « A spiral 2D phased array for 3D imaging », in *Ultrasonics Symposium, 1999. Proceedings. 1999 IEEE*, Caesars Tahoe, NV, USA, 1999, vol. 2, p. 1271–1274 vol.2.

[8] Chi Hyung Seo et J. T. Yen, « A 256 x 256 2-D array transducer with row-column addressing for 3-D rectilinear imaging », *Ultrasonics, Ferroelectrics and Frequency Control, IEEE Transactions on*, vol. 56, n°. 4, p. 837–847, 2009.

[9] N. N. Lee, R. W. O'Rourke, J. Cheng, et P. D. Hansen, « Transthoracic hepatic radiofrequency ablation », *Surg Endosc*, vol. 18, n°. 11, p. 1672–1674, oct. 2004.

[10] J. A. Jensen, « FIELD: A Program for Simulating Ultrasound Systems », *10TH NORDICBALTIC CONFERENCE ON BIOMEDICAL IMAGING VOL 4 SUPPLEMENT 1 PART 1 351–353*, vol. 34, n°. Supplement 1, Part 1, p. 351–353, 1996.

[11] J. A. Jensen et N. B. Svendsen, « Calculation of pressure fields from arbitrarily shaped, apodized, and excited ultrasound transducers », *IEEE Transactions on Ultrasonics, Ferroelectrics and Frequency Control*, vol. 39, n°. 2, p. 262–267, mars 1992.

[12] A. Austeng et S. Holm, « Sparse 2-D arrays for 3-D phased array imaging - design methods », *Ultrasonics, Ferroelectrics and Frequency Control, IEEE Transactions on*, vol. 49, n°. 8, p. 1073–1086, 2002.

[13] B. Diarra, H. Liebgott, P. Tortoli, et C. Cachard, « 2D matrix array optimization by simulated annealing for 3D hepatic imaging », *IEEE International Ultrasonics Symposium*, Orlando, Florida, USA, p. in press, oct-2011.

[14] G. R. Lockwood et F. S. Foster, « Optimizing the radiation pattern of sparse periodic two-dimensional arrays », *IEEE Transactions on Ultrasonics Ferroelectrics and Frequency Control*, vol. 43, n°. 1, p. 15–19, janv. 1996.

[15] M. Karaman, I. O. Wygant, O. Oralkan, et B. T. Khuri-Yakub, « Minimally redundant 2-D array designs for 3-D medical ultrasound imaging », *IEEE Trans Med Imaging*, vol. 28, n°. 7, p. 1051–1061, juill. 2009.

[16] A. Trucco, « Thinning and weighting of large planar arrays by simulated annealing », *IEEE Trans. Ultrason., Ferroelect., Freq. Contr.*, vol. 46, n°. 2, p. 347–355, mars 1999.

[17] P. Yang, B. Chen, et K.-R. Shi, « A novel method to design sparse linear arrays for ultrasonic phased array », *Ultrasonics*, vol. 44, n°. Supplement 1, p. e717–e721, déc. 2006.

[18] J. E. Gubernatis, « Marshall Rosenbluth and the Metropolis algorithm », *Phys. Plasmas*, vol. 12, n°. 5, p. 057303, 2005.

[19] S. Kirkpatrick, C. D. Gelatt, et M. P. Vecchi, « Optimization by Simulated Annealing », *Science*, vol. 220, n°. 4598, p. 671 –680, mai 1983.

[20] M. A. Chitre et J. R. Potter, « Optimization and Beamforming of a Two Dimensional Sparse Array ».

[21] P. Chen, B. Shen, L. Zhou, et Y. Chen, « Optimized simulated annealing algorithm for thinning and weighting large planar arrays », *J. Zhejiang Univ. - Sci. C*, vol. 11, n°. 4, p. 261–269, avr. 2010.

[22] R. O. Nielsen, *Sonar Signal Processing*. Artech House Publishers, 1991.

[23] G. Cardone, G. Cincotti, P. Gori, et M. Pappalardo, « Optimization of wide-band linear arrays », *IEEE Trans Ultrason Ferroelectr Freq Control*, vol. 48, n°. 4, p. 943–952, juill. 2001.

[24] A. Trucco, « Weighting and thinning wide-band arrays by simulated annealing », *Ultrasonics*, vol. 40, n°. 1–8, p. 485–489, mai 2002.